Pozzi M. Magnetic plucking of piezoelectric bimorphs for a wearable energy harvester. *Smart Materials and Structures* 2016, 25(4).

Magnetic plucking of piezoelectric bimorphs for a wearable energy harvester

Michele Pozzi

School of Mechanical and Systems Engineering, Newcastle University, Newcastle upon Tyne, NE1 7RU, UK

E-mail: michele.pozzi@newcastle.ac.uk

Abstract. A compact and low-profile energy harvester designed to be worn on the outside of the knee-joint is presented. Frequency up-conversion has been widely adopted in recent times to exploit the high frequency response of piezoelectric transducers within environments where only low frequencies are present. Contactless magnetic plucking is here introduced, in a variable reluctance framework, with the aim of improving the mechanical energy transfer into the transducers, which is sub-optimal with contact plucking. FEA and experiments were used to design an optimal arrangement of ferromagnetic teeth to interact with the magnets fixed to the piezoelectric beams. A prototype was made and extensively tested in a knee-joint simulator controlled with gait data available in the literature. Energy and power produced were measured for walking and running steps. A power management unit was developed using off-the-shelf components, permitting the generation of a stable and regulated supply of 26 mW at 3.3 V during walking. Record levels of rectified (unregulated) electrical power of over 50 mW and 70 mW per walking and running steps, respectively, were measured.

Keywords: Energy Harvesting, frequency up-conversion, magnetic plucking, piezoelectric bimorph, wearable energy harvester

1. Introduction

Energy harvesting, the process of converting otherwise untapped environmental energy to operate low power devices, has been constantly growing in the past three decades. Initially seen as a fit-and-forget solution for monitoring processes, structures and the environment, it is set to enter the consumer market due to the ubiquitous presence of wearable devices, designed to monitor physical workouts and health parameters and even sleep. A truly friendly 24/7 monitoring device must be self powered. For the first decade of its existence, the main focus of energy harvesting, originally known as energy scavenging, has been environmental vibrations [1,2], although all forms of environmental energy have probably been investigated at some point. Whereas light and thermal gradients hold potential also for wearable energy harvesting, vibrations are not as present in humans as they are in machinery. For this reason, motion-based wearable energy harvesters (EHs) are more likely to use changes of tilt [3,4], relative motion between two parts [5,6] or accelerations sufficiently large to warrant energy harvesting [7,8].

Human motion, be it tilt, inertial or relative motion of two parts, is typically rather slow in comparison to the speeds required by electromagnetic generators or the capabilities of piezoelectric transducers. Although both solutions find active supporters among researchers, both also need clever design solutions to couple the available energy efficiently into the transducer/generator. The idea of frequency-up-conversion has now become mainstream and is typically implemented via impact [8–10] or plucking [11,12]. Impact excitation implies an instantaneous transfer of momentum into the transducer and is mathematically represented by differential equations (DEs) with initial conditions (ICs) which are zero on the displacement but non-zero on the velocity. Plucking excitation implies a slow deflection of the transducer followed by its sudden release and is mathematically represented by DEs with ICs which are zero on velocity but not on displacement. Naturally, in real practice, excitation will have both characters: impact will have finite duration so that some deflection is present upon loss of contact; in plucking the transducer may have non-zero velocity when it loses contact with the plectrum. Both these techniques, when applied to piezoelectric devices via mechanical contact, could potentially lead to damage of the brittle material. For this reason, contactless interaction between magnets has been investigated by, for example, Luong and Goo [13] and Pillatsch et al. [14]. Magnetic plucking with contact has also been employed, by making the tip of the transducer stick to a magnet [11,15,16]; this has the advantage that the force applied to the transducer is limited by the magnetic force at contact and could be useful to limit the stress in a piezoelectric material in the case the transducers are bimorphs. It is worth noting that magnetic interaction has also been used to widen the bandwidth of vibrational harvesters by introducing non-linearities and chaotic behaviour [17–19].

Although mechanical plucking via direct contact of a plectrum has the potential to damage the piezoelectric ceramics, appropriate mitigating measures could be easily

implemented. Therefore, in the view of the author, the fact that mechanical plucking via a plectrum is very sensitive to manufacturing accuracy is more important: the common occurrence of unclean, inefficient plucking actions was demonstrated in [20]. In the same paper it was estimated that this factor on its own could account for a loss of over 40% in energy output. It was shown that whereas the piezoelectric beam can be deflected consistently, much energy may be wasted when it is released since the plectrum that deflects it, also impedes the free initial movement of the bimorph. Magnetic plucking has the potential to avert this issue as contact friction is absent. Magnetic forces can still provide sharp plucking, as they vary rapidly with distance at short range.

The present work builds upon the knee-joint energy harvester presented by Pozzi et al. in [21] – a more compact and actually wearable redesign of the Pizzicato harvester developed earlier [6,20]. Mechanical plectra were removed and replaced with a magnet-tooth arrangement to implement contactless plucking. This sole modification yielded a tenfold increase in energy output, as reported in the following sections.

2. Experimental methods

The focus of this paper is the energy harvester shown in figure 1. It is designed to be worn on the outside of the knee-joint [21]: two brackets fixed to shin and thigh transmit the natural rotation of the joint causing the relative rotation of the central hub, holding the piezoelectric bimorphs, and the casing, carrying the iron plectra. The bimorphs were obtained by cutting with a diamond saw commercially available rectangular bimorphs (see figure 1). These series bimorphs are made of a 130 μm-thick brass layer sandwiched between two PZT-5H active layers, to give a total thickness of 380 μm. The wavy area in the figure had the external electrodes removed and was fixed into the aluminium hub with adhesive. A pair of permanent magnets was attached to each bimorph with their magnetic axis along the beam but in anti-parallel configuration. The magnets are (rounded) cubes of 3×3×3 mm^3 volume and made of N42 neodymium-based material. Other researchers have used permanent magnets at both ends either in attractive or repulsive configuration. Here, as more flexibility was desired for the geometry of the teeth, the latter were machined out of soft iron via CNC milling. For reasons discussed in later sections, there are 65 teeth, 0.5 mm wide (hoop direction), with a pitch of 3.5 mm and at a design distance of 0.5 mm from the tip of the bimorphs. For bench testing, the case and teeth are fixed to the stator of a servo-motor, whereas the central hub with the bimorphs is driven by the rotor. The motor can be computer controlled to accurately reproduce the human gait. For the tests in this paper, control curves are generated from experimental data on gait reported by Diedrich and Warren [22].

Each piezoelectric beam has two wires connected to it, which take the generated charges to individual full bridge rectifiers (Bourns CDNBS04-B08200) surface mounted on a custom PCB. The outputs of all bridges are brought together to form a parallel arrangement of generators. When measuring the energy produced by the piezoelectric elements directly (i.e. after rectification but without the PMU described later), the

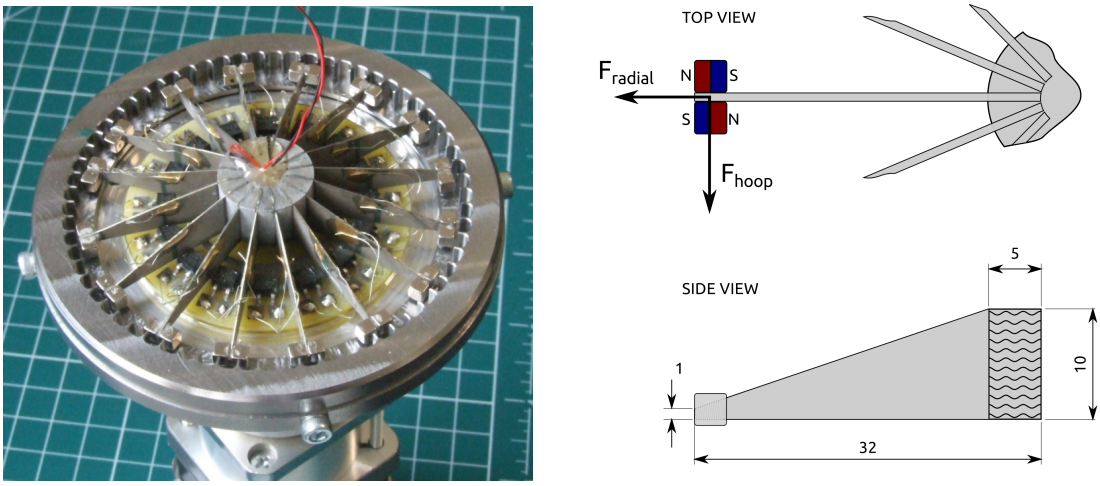

Figure 1. (left) the energy harvester mounted on the servo motor and (right) cutaway top and side view of a bimorph, including orientation of the magnets (sketch not to exact scale). The wavy pattern indicates the area fixed into the hub. Dimensions are in mm.

total output is dissipated over a 14.7 kΩ resistor (a 14.9 kΩ discrete resistor in parallel with the nominal input resistance of the DAQ). The DAQ is a National Instruments NI 9221, capable of ±60V input at 12 bits.

A Power Management Unit (PMU) was developed around the Linear Technology chip LTC3588-1 and configured for a 3.3 V output. This was used as an alternative load for the EH to test the potential for driving a real load requiring regulated supply.

Unless otherwise specified, data are given in the following as mean of the stated number of values; the uncertainties reported correspond to a 95% confidence level using the t-Student distribution.

3. Modelling methods

Finite Element Analysis (FEA) was conducted in Comsol Multiphysics with the AC/DC module using static magnetic fields. The objective was to estimate the interaction forces in the hoop and radial directions between magnets on the bimorphs and fixed iron teeth.

The geometry is modelled in three dimensions and is made of two fixed magnets (cubes of N42 composition, edges of 3 mm) with antiparallel orientation and spaced 0.5 mm (the thickness of the bimorph). At a set distance from them and facing them, a tooth or set of teeth was rotated around a circle of radius 36.5 mm. Everything was immersed in air. Only half geometry was actually modelled, exploiting the inherent planar symmetry (see figure 2).

Starting with a normal mesh, this was progressively refined to select the optimal mesh size. Convergence of the calculated forces was noted with further refinement. In order to save computing resources, refinement was concentrated in the region between teeth and magnets, which plays the greater role in the magnetic interaction (see figure 2).

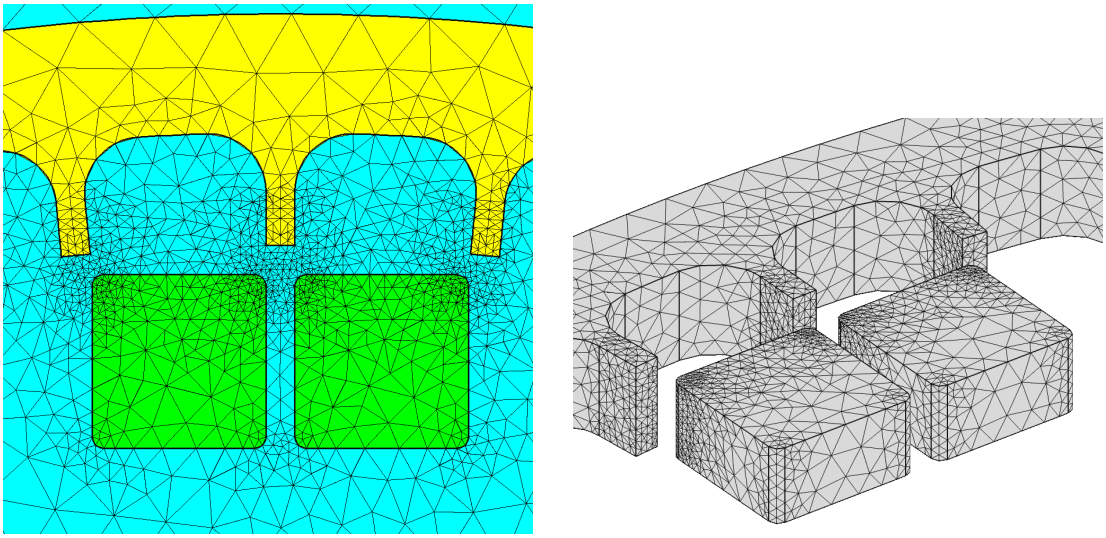

Figure 2. Geometry and mesh used in the FEM. The images are specific to 65 teeth-spacing and a distance magnet-tooth of 0.50 mm. The arrangement shown represents the origin of the rotation, i.e. angle = 0°. Note that the piezoelectric beam between the magnets was not modelled and is therefore not visible

Initially, a single tooth was modelled, located at a selected set of distances from the magnets (0.25, 0.50 and 0.75 mm). Its dimensions were guided by experimental tests performed earlier, which indicated that a width (along the arc) of 0.5 mm was optimal for those magnets.

Finally, a set of teeth was modelled, to explore their collective effect and select their optimal spacing. Starting with a total of 65 teeth (corresponding to an angular distance of 5.54° or 3.5 mm along the arc, which is the distance between the magnets' centres) two other spacings were investigated at either end: 50 teeth (7.2° or 4.6 mm) and 93 teeth (3.9° or 2.5 mm). All configurations were tested for the same set of magnet-tooth distances.

4. FEA Results and Discussion

The components of the magnetic force between the pair of magnets and a single tooth are plotted in figure 3. The objective is to show the effect of relative position magnet-tooth during rotation and for a selection of radial distances. The hoop component will cause bending of the bimorph, whereas the attractive radial force induces (modest) tension in it. In the following discussion, an angle of 0° means that the tooth is aligned with the bimorph that would be present between the two magnets. When the tooth is sufficiently far (angle = -10°), the hoop component is almost zero; the radial component is already attractive because the tooth is protruding from a continuous ferrous ring. At -5°, we observe the peak of lateral force, which quickly drops to zero at about -3° when the tooth is aligned with the middle of the first magnet. In approximately the same position, we observe the maximum attractive force. The hoop force then changes sign as the tooth is

still attracted mostly by the same magnet, which is moving away. Another zero crossing for the hoop force is observed when the angle is zero, as the tooth is equally attracted by the two magnets. This also correspond to a minimum in radial force because the magnets present opposite polarity towards the tooth and the field lines will close onto each other very near the magnets. Beyond 0°, the behaviour is symmetric (and in fact rotation above 0° was not modelled, but the data simply reflected to complete the graphs reported).

The key results of the FE analysis are the extremes of the hoop force to which the magnets on the bimorph are exposed. They represent the maximum bending forces applied to the bimorph, and therefore the strength of the plucking actions. The FEA model assumes that tooth and magnets are constrained to the set rotation. In experiments, the large hoop component seen in figure 3 at -5°, for example, will bend the bimorph towards the nearby tooth until it will be almost locked to face the tooth as rotation continues. Beyond 0°, the attraction from the other magnet prevails and the bimorph locks on the latter. The slope of the force vs. angle curve determines how tightly locked the bimorph is. The result is that three dissimilar plucking actions are produced: from free to the first magnet, on to the second magnet, from this to free. Increasing the distance magnet-tooth decreases the peak values of the force, as expected. It also reduces the asymmetry of the curve: the first peak (at -5°) is almost exclusively determined by the first magnet, the second one (at -1.2°) is the combined effect of both magnets, offering opposite polarities and pulling in opposite directions. The absolute value of both peaks decreases with increasing distance, but the second one is less affected because the two opposing forces decrease similarly with distance.

Figure 4 explores the effects of both magnet-tooth distance and number of teeth (i.e. spacing between teeth). The force components are modelled and plotted over a whole period: at 0°, a tooth is midway between the magnets; at the end of the period, the next tooth will be in the same position. The teeth appear to act in pairs, closing the magnetic circuit produced by the magnets facing them. Regarding the hoop force, only two peaks are observed, the magnets attracted to one or the other pair of teeth, according to which is the closest. Similarly, the radial force only has a minimum, when each magnet is attracted by the tooth facing it. In fact, these observations are strictly valid only for 50 and 65 teeth; with 93 teeth the interaction force is almost constant during rotation, except for the smallest distance.

These results show that large hoop forces are obtained both with 50 and 65 teeth. The selected number of teeth was 65 as the lower number (namely 50) gave similar forces but on a longer period, which means fewer plucking actions per revolution. The largest number of teeth (93) was obviously discarded as minimal hoop forces are produced. The reason is that the teeth are so close to each other as to appear almost as a continuum.

The magnet-tooth distance of 0.5 mm was selected for the prototype as it results in a maximum bending force just over 0.2 N applied at the tip of the bimorph (figure 4), which was shown via FEA and analytical calculations to produce a static deflection of about 0.6 mm with a maximum longitudinal strain of $4 \cdot 10^{-4}$ in the piezoelectric material.

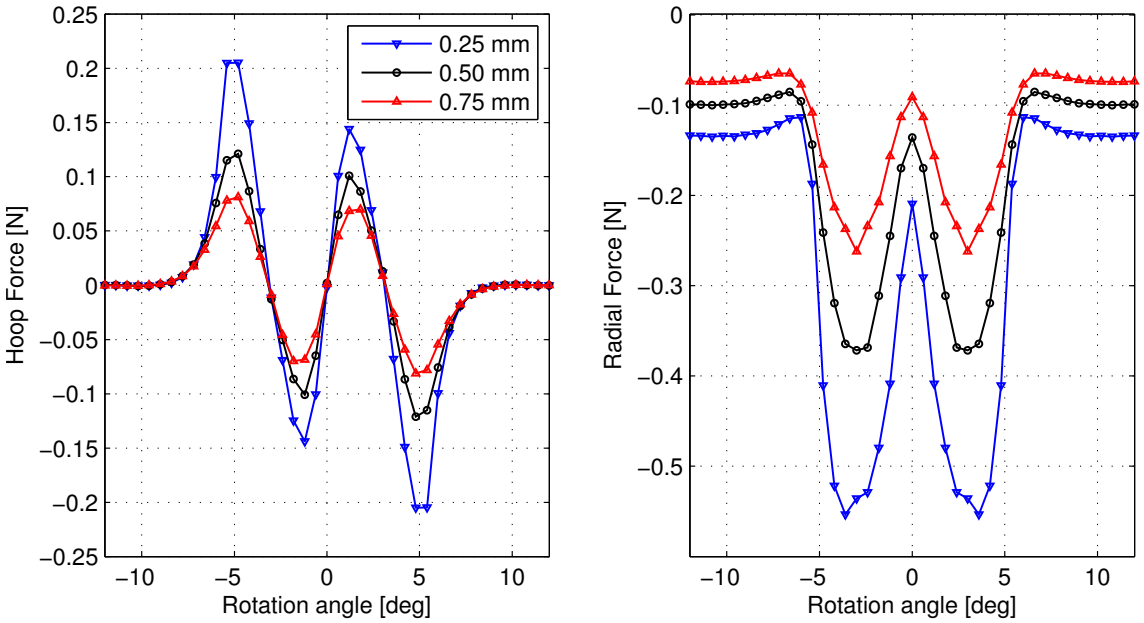

Figure 3. Effect of radial distance on the magnet-tooth interaction with a single tooth

This is a good value to ensure a large mechanical energy transfer together with a long life of the piezoelectric material – the manufacturer's recommended operating conditions imply a maximum strain of about $5{\cdot}10^{-4}$. More energy would have been obtained with a distance of 0.25 mm, but service life would be shortened and manufacturing and mounting tolerances would have made a potentially destructive direct contact between magnets and teeth quite possible.

5. Experimental results and Discussion

The performance of the device was evaluated in several scenarios. The movement of the hub was either at constant speed or reproducing walking or running gait. Firstly, a single bimorph was provided with magnets and a single tooth was used for plucking. Then the complete device, with all magnets installed and the ring with 65 teeth, was used; simply rectified voltage was recorded as well as the output from the PMU. Finally, one bimorph was disconnected from its rectifier to only record its raw output when plucked by the full ring of teeth.

5.1. One bimorph and one tooth

Initial experiments were carried out with the aim of determining the effect of the shape of the tooth. It was found that the teeth leading to higher energy generation offered a rectangular face to the magnets, with the same height of the magnet (i.e. 3 mm) or higher and a width of around 0.5 mm; wider teeth were causing less sharp plucking, consequently leading to a lower energy generation. Note that in all cases the radial dimension of the tooth was much larger than the other two dimensions. Another set of

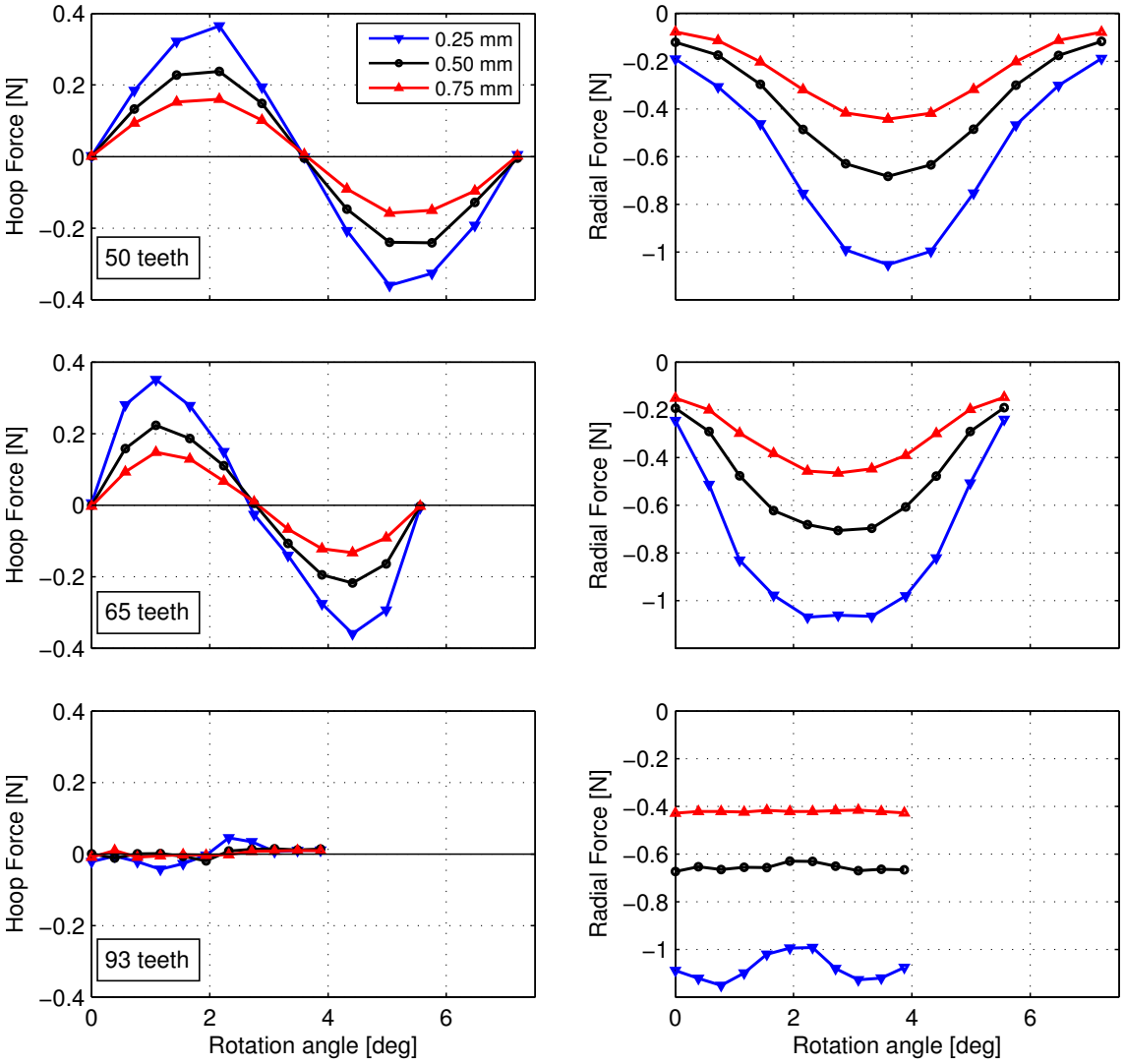

Figure 4. Effect of magnet-tooth distance and number of teeth on the interaction magnets-teeth.

experiments was directed at determining the dependence of energy on distance between magnets and a 3 mm×0.5 mm iron tooth. These data are summarised in Table 1. For each distance, 8 plucking actions were recorded, 4 in the Forward direction and 4 in the Reverse direction.

These data show that energy generation is greatly influenced by the distance between tooth and magnets, with a 50-fold increase as the distance is reduced from 1.4 to 0.5 mm. This is in agreement with the FEA results in figure 3. It is clear from data in the table that there is a higher generation for reverse than forward direction. This is unexpected as the arrangement was intended to be symmetrical. The asymmetry could be due to inaccuracies in the attachment of the magnets to the bimorph or in the tooth. It is also not clear why the difference did not appear at intermediate distances (0.8 and 0.7 mm). The discrepancy is therefore thought to be due to some uncontrolled factor in the set-up. Experiments were also performed to investigate the effect of transit

Table 1. Effect of magnet-tooth distance in energy generation. The column Direction indicates if the encounter happened in the Forward or Reverse direction.

Distance [mm]	Direction	Energy/pluck [μJ]
1.4	FWD	1.5 ± 0.2
	REV	2.6 ± 0.3
1.2	FWD	3.0 ± 0.4
	REV	5.3 ± 0.2
1.1	FWD	4.7 ± 0.5
	REV	7.9 ± 1.1
0.8	FWD	30 ± 2
	REV	31 ± 1
0.7	FWD	41 ± 2
	REV	40 ± 1
0.6	FWD	60 ± 6
	REV	78 ± 6
0.5	FWD	78 ± 4
	REV	110 ± 10

speeds, within the range 0.09 to 0.29 m/s. The modulus of the relative velocity at the time of encounter had no statistically significant effect.

5.2. Complete device

Figure 5 and figure 6 reproduce data obtained with the complete device: in the first one, one single step of walking gait was produced 8 times; in the second, 5 consecutive running steps were produced 5 times. The figures show with a thick line the mean of the test runs; the minimum and the maximum calculated at each point in time are shown with lighter lines. Note that the voltage signal is occasionally clipped at 62.4 V, the maximum measured by the DAQ.

Figure 5 shows that, during a normal step, energy is mostly generated in four bursts, corresponding to the periods where the knee-joint undergoes significant rotation. A similar behaviour is noticed in the running gait (figure 6). Although these figures suggest a large variation in the voltage produced at any specific point, it must be remembered that the extrema are calculated instantaneously, point-by-point. Analysing a larger number of experimental measurements (27 walking steps and 26 running steps), the total rectified energy produced is calculated as 46.5±1 mJ per walking step and 49.4±2 mJ per running step.

To establish the capability of the harvester to power a real load, its output was fed to the PMU to supply stabilised direct current at 3.3 V. Since the output of the PMU was connected to a 550 Ω resistor, the system was required to supply a constant regulated power of 20 mW. Figure 7 demonstrates that this was achieved with two configurations of the PMU. For the top graph, a 47 μF electrolytic capacitor was placed in parallel to the PMU input, therefore storing the charges as they are available at the

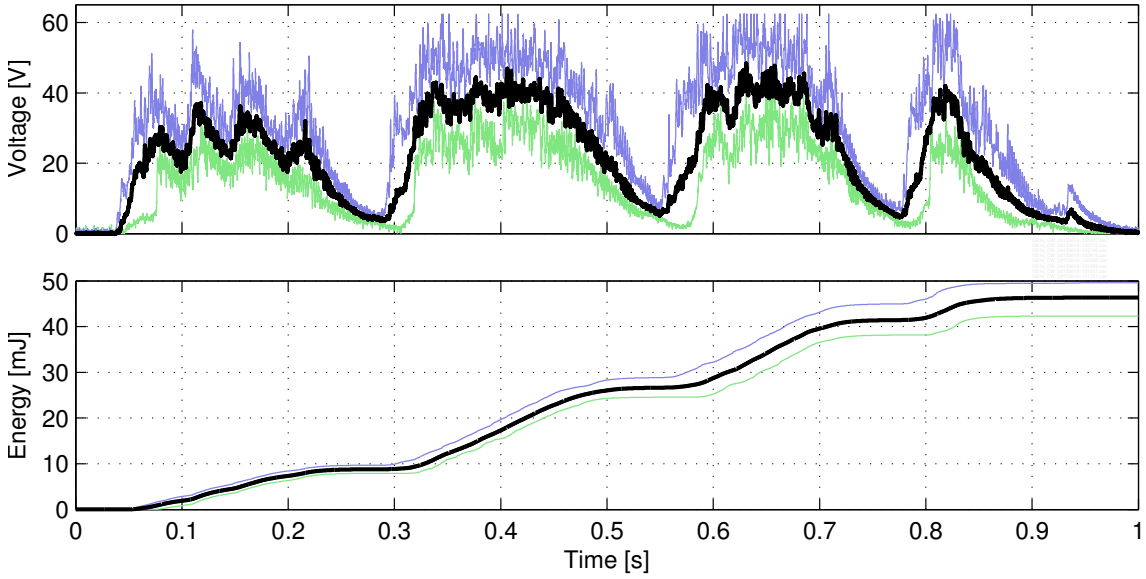

Figure 5. voltage output and cumulative energy with one step at walking gait with all 16 bimorphs active. The thick line represent the mean of 8 test runs, whereas the lighter lines are point-by-point minima and maxima of the same.

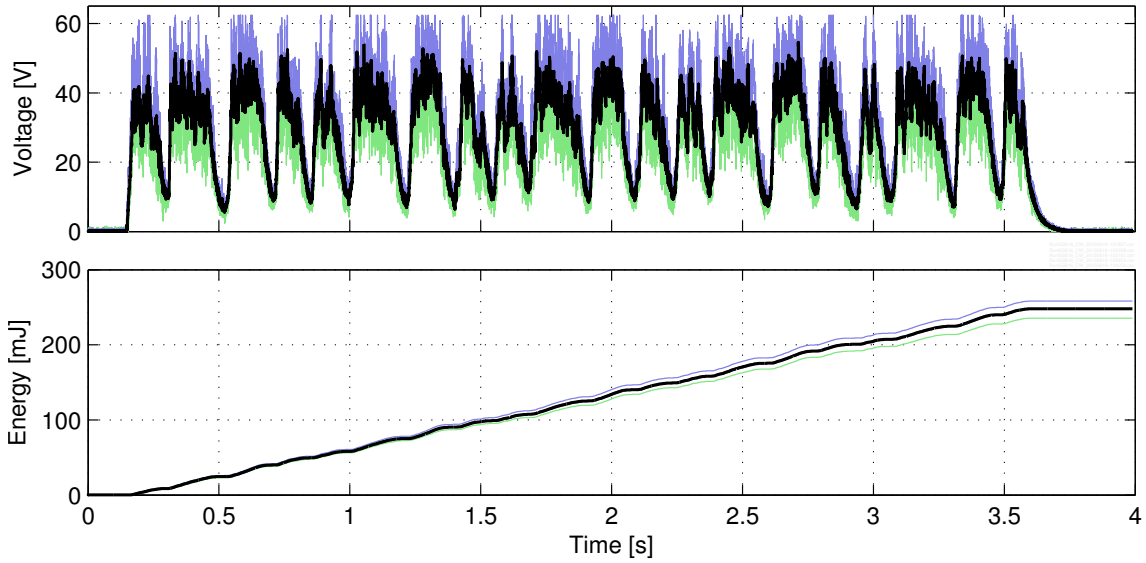

Figure 6. voltage output and cumulative energy with five running steps and all 16 bimorphs active. The thick line represent the mean of five test runs, whereas the lighter lines are point-by-point min and max of the same.

rectifiers' outputs; for the bottom graph, such capacitance was increased to 517 μF. For both tests, the gait for 4 walking steps was commanded 4 times, giving a total of 16 walking steps; a brief pause is introduced by the D/A card after each sequence of 4 steps and produces a slight dip in the input voltage. The resistive load is connected to the output of the PMU 1 s after the voltage rises to 3.3 V (Power Good), to ensure sufficient charges are stored in the input capacitors. Note that the input capacitors charge up to

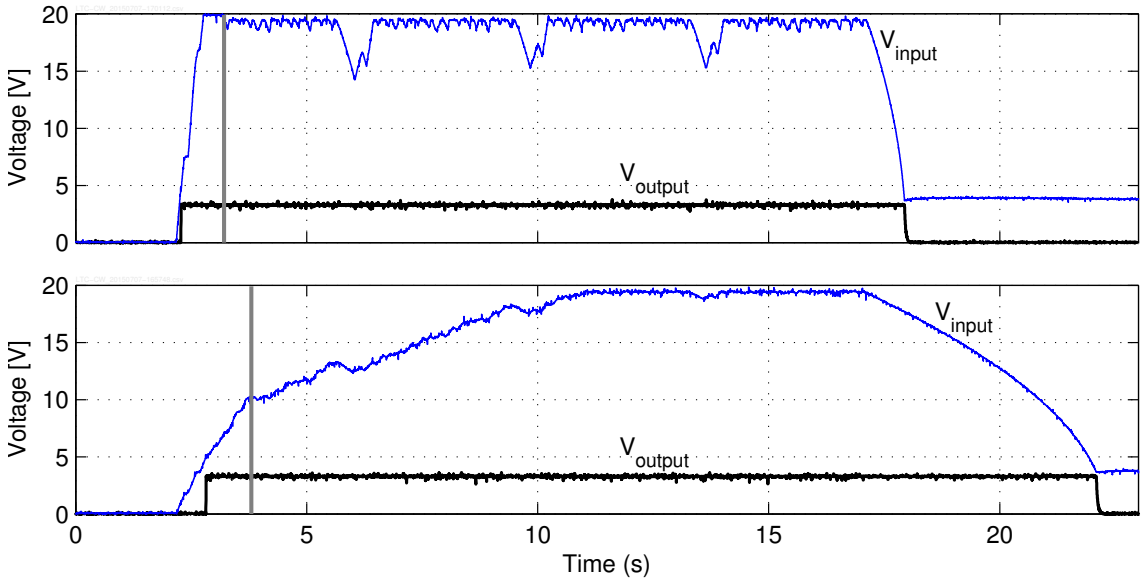

Figure 7. Regulated 3.3 V DC output voltage from the PMU and input to the PMU. Top graph with 47 μF at input, bottom graph with 517 μF. Harvester driven with 4 sequences of 4 walking steps each. The vertical lines indicate when the resistive load was connected to the PMU's output.

a maximum of 20 V as Zener diodes within the LTC3588-1 clamp the input voltage to this value.

5.3. One bimorph active

A series of experiments was carried out to isolate the contribution of a single bimorph from the combined signal. The wires of one of the bimorphs were disconnected from its bridge rectifier and directly connected to the same resistive load used for the whole device, equivalent to 14.7 kΩ; the output voltage across this load was then sampled. As in the previous section, the harvester had the ring of iron teeth mounted; the otherwise unmodified hub was driven at either constant-speed or with walking or running gaits. Full revolutions were executed at a selection of constant speeds, ranging from 1 rev/s to 0.1 rev/s. The hub was driven in both directions alternatively, collecting 6 runs at each speed (3 clockwise and 3 counter-clockwise). When testing the effect of gait, 16 steps were measured for running and 14 for walking; these were equally split between the two directions and conducted at the natural speeds of 0.88 s/step for walking and 0.69 s/step for running. In this case, reversing the direction is akin to wearing the device on the other leg; whereas magnets-teeth pass each other in alternating directions within each gait. The measured energy and power are collated in Table 2. Time domain data for speeds of 0.1 rev/s and 0.5 rev/s are reproduced in figure 8 and figure 9, respectively. The top graphs show the raw, non-rectified voltage at the electrodes of the bimorph connected to a 14.7 kΩ equivalent resistance; the corresponding energy generated is in the lower graphs. Smaller graphs on the right are used to highlight details of the data,

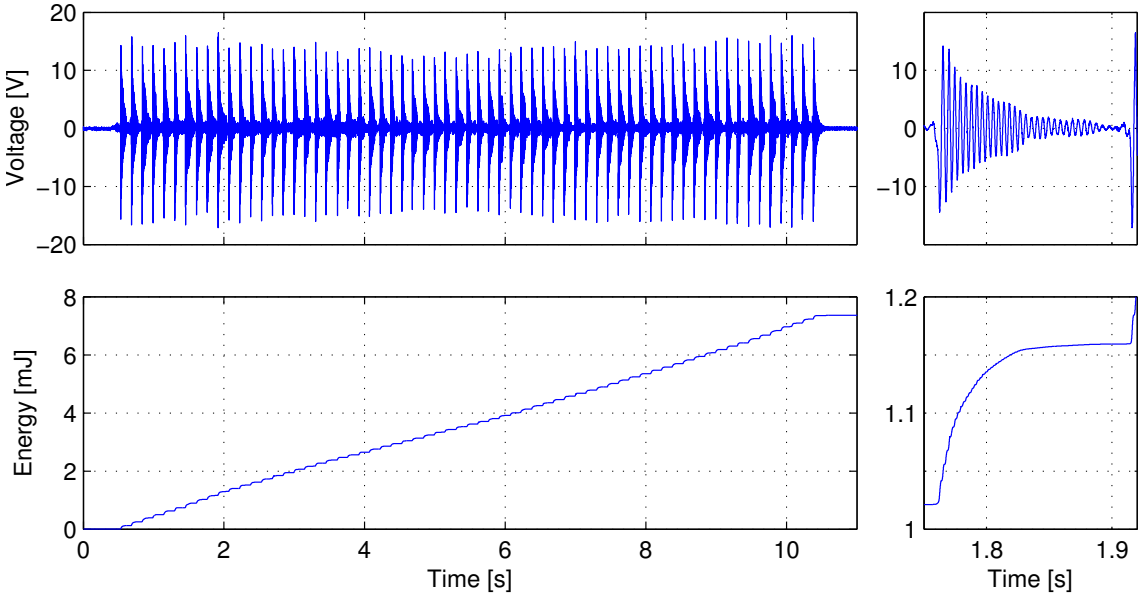

Figure 8. Voltage and cumulative energy produced by a single bimorph over a full revolution at constant speed of 0.1 rev/s. The smaller plots on the right highlight a detail.

Table 2. energy and power produced by one bimorph in one revolution at a selection of speeds or in one step at the specified gait.
Confidence intervals are not given for CW and CCW separately due to the low number of data points.

Commanded motion	Energy/rev CW [mJ]	Energy/rev CCW [mJ]	Energy/rev [mJ]	Power [mW]
$10s/rev$	7.2	7.4	7.3 ± 0.2	0.73 ± 0.02
$5s/rev$	7.6	7.3	7.4 ± 0.2	1.49 ± 0.04
$3s/rev$	7.4	7.3	7.3 ± 0.2	2.44 ± 0.07
$2s/rev$	6.3	6.6	6.5 ± 0.2	3.2 ± 0.1
$1s/rev$	3.9	4.2	4.1 ± 0.2	4.1 ± 0.2
walking	2	2.2	2.1 ± 0.1	2.3 ± 0.1
running	2.1	2.1	2.1 ± 0.1	3.0 ± 0.2

by zooming into a briefer time interval. Similarly, voltage and cumulative energy for typical walk and run gaits are plotted in figure 10 and figure 11, respectively.

6. Further Discussion

Figure 7 shows that with the smaller capacitance, the output is maintained at 3.3 V on the load for 14.7 s, outputting 291 mJ of regulated energy; with the larger capacitance, the PMU output is delayed an extra 0.6 s, but remains valid for 18.3 s, outputting 362 mJ (so 24% more energy). As the 16 walking steps last approximately 14 s in total, 26 mW of regulated power can be generated. Comparing these values with the rectified

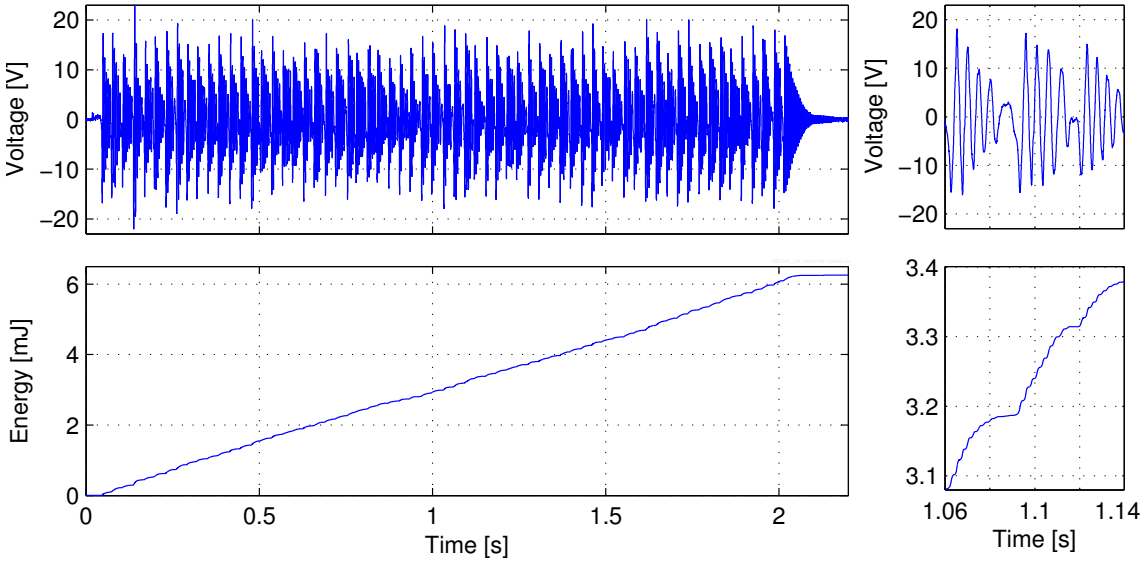

Figure 9. Voltage and cumulative energy produced by a single bimorph over a full revolution at constant speed of 0.5 rev/s. The smaller plots on the right highlight a detail.

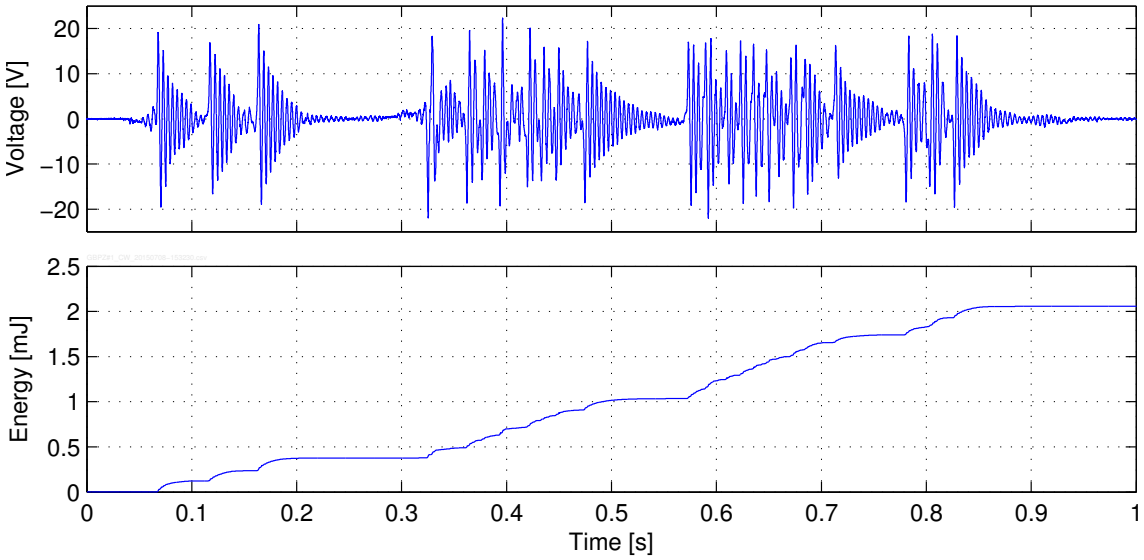

Figure 10. Voltage and cumulative energy produced during a walking gait by a single bimorph.

energy produced in one walking step (figure 5), the observed efficiency of the PMU is at best 50%. The fixed output load means that any excess power produced by the harvester has to be dissipated (in the Zener diodes). The larger input capacitor simply stores some energy and makes it available when the harvester has stopped operating. In application, a battery would be connected to the output of the PMU, so as to provide ample storage at nearly constant voltage and low-impedance. This configuration would permit more of the energy available at the input of the PMU to be brought at the right voltage and stored. The overall efficiency of the system would moderately improve.

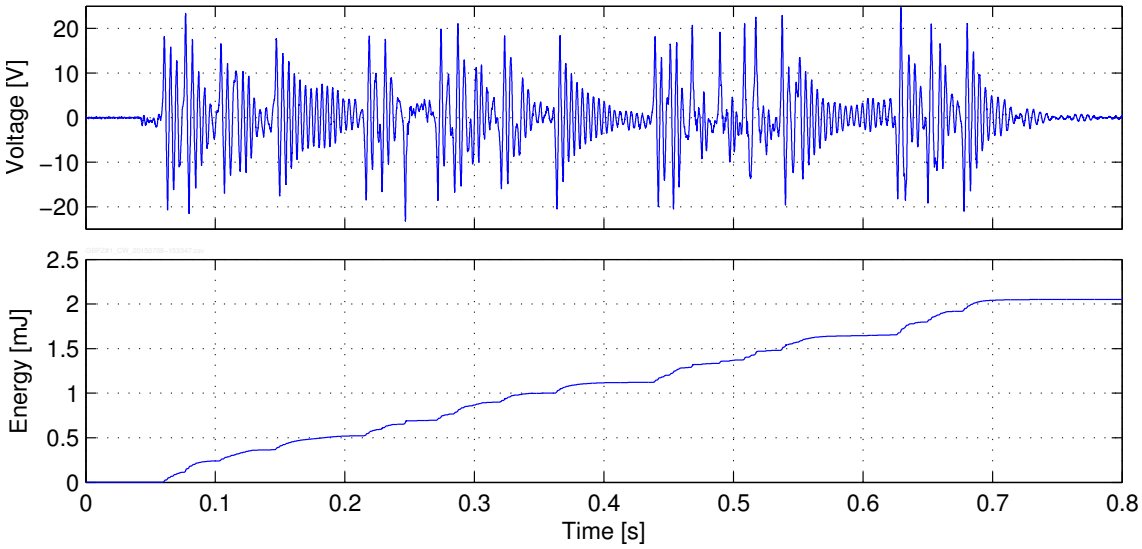

Figure 11. Voltage and cumulative energy produced during a running gait by a single bimorph.

Table 3. summary of performance of the knee-joint harvester. Data with mechanical plucking (Kapton and steel plectra) are taken from [21]

Conditions	Power [mW]
Walk, magnetic, rectified	52.8 ± 1
Run, magnetic, rectified	71.6 ± 3
Walk, magnetic, regulated	≈ 26
Walk, 80 steel plectra, rectified	5.4 ± 0.3
Run, 80 steel plectra, rectified	7.5 ± 0.5
Walk, 78 Kapton plecta, rectified	1.03 ± 0.08
Walk, 78 Kapton plecta, regulated	0.34

In one respect, magnetic plucking is strikingly different from contact plucking. Table 2 shows that the energy produced by magnetic plucking is reduced when the plucking frequency exceeds a threshold value. It is constant up to 22 plucks/second and a decline is observed starting at about 32 plucks/s. Taking the low speed/low frequency as reference, it is possible to speak about a decrease of effectiveness brought about by too high a plucking frequency. The root cause is evident by comparing figure 8 and figure 9: in the former, vibrations induced by a plucking action have the time to naturally die down, so that all associated mechanical energy is converted to electrical. In the latter, a new magnet-tooth interaction disrupts the vibrations induced by the previous one while they are still generating significant electrical power. It remains true that higher revolution speeds yield higher output power (table 2). The decrease in energy generation with increasing plucking frequency is in stark contrast with what previously observed in the case of mechanical plucking [20].

Comparing data reported in Table 2 with figure 5, it emerges that the isolated

bimorph generated 2.1±0.1 mJ during one walking step, whereas the figure indicates that on average each bimorph contributes 2.9±0.1 mJ. Subsequent experiments showed that the difference is mostly due to the fact that the resistive load of 14.7 kΩ, optimally selected for the full device, is in fact a poor choice in the case of a single bimorph: increasing the load to 74.9 kΩ produced voltages exceeding 62.4 V and over 3.7 mJ per walking step, before rectification.

The huge improvement brought about by the introduction of magnetic plucking can be appreciated from Table 3. The same hub and bimorphs were tested with mechanical plucking via plectra made of Kapton or steel [21] and a maximum power of 7.5 mW was obtained with steel plectra and running gait. The replacement of contact plucking with magnetic plucking and the changed dynamics due to the added tip mass has brought this value up to almost 72 mW; likewise, a walking gait that could generate 5.4 mW can now produce almost 53 mW of rectified electrical power.

7. Conclusions

The low profile knee-joint energy harvester has been upgraded by replacing contact plucking with contactless magnetic plucking. Neodymium-based N42 magnets of size 3×3×3 mm^3 have been fixed to the tip of the bimorphs in anti-parallel arrangement. A variable reluctance principle was applied, permitting great flexibility in the design of plucking teeth. FE models and experiments have been used in concert to design the stationary ferromagnetic teeth for optimal performance. The selected teeth are 0.5 mm wide and are placed at a design distance of 0.5 mm from the magnets. The optimal spacing between the teeth matches the distance between the magnets' centres.

With the harvester mounted on a knee-joint simulator, driven by gait data from literature, rectified electrical power of almost 53 mW (walking) and almost 72 mW (running) were measured. This represents an almost ten-fold improvement over mechanical plucking [21]. Although it was not possible to measure the mechanical input power to calculate the overall efficiency, it is worth noting that FE results suggest that a torque below 0.12 Nm would be sufficient to operate the harvester. Since the torque produced by the knee during walking varies between -20 Nm and 40 Nm [23], the additional effort required would be minimal.

Furthermore, calculations suggest that normal service life can be expected, as the design strain imposed to the piezoelectric material is within manufacturer's recommendation. Extensive experimental testing to date has not shown signs of degradation of performance, although manufacturing imperfections may be subjecting some bimorphs to higher than design strains.

A power management unit delivering regulated current was developed using off-the-shelf components and demonstrated an efficiency of 50%. Some reasons for this disappointing figure have been offered and discussed with the conclusion that there is scope for improvement on this front.

The device presented here demonstrates the potential of piezoelectric energy

harvesting based on up-conversion via magnetic plucking for wearable applications. The variable reluctance approach, as opposed to matching permanent magnets, reduces cost and affords valuable design flexibility. The same principle can be applied to other joints on the body. More in general, any environment with relative movement between parts (linear or rotational) can benefit from this approach. Even in the absence of relative motion, inertial effects can be exploited to fit this technique to other areas of the body or environments.

References

[1] Williams C B and Yates R B 1996 Analysis of a micro-electric generator for microsystems Sens. Actuators Phys. 52 8–11

[2] Roundy S, Wright P K and Rabaey J M 2004 Energy Scavenging for Wireless Sensor Networks with Special Focus on Vibrations (Boston, MA: Springer US)

[3] Shukla R and Bell A J 2015 PENDEXE: A novel energy harvesting concept for low frequency human waistline Sens. Actuators Phys. 222 39–47

[4] Pillatsch P, Yeatman E M and Holmes A S 2012 A scalable piezoelectric impulse-excited energy harvester for human body excitation Smart Mater. Struct. 21 115018

[5] Paradiso J A and Feldmeier M 2001 A Compact, Wireless, Self-Powered Pushbutton Controller Proceedings of the 3rd International Conference on Ubiquitous Computing UbiComp '01 (London, UK, UK: Springer-Verlag) pp 299–304

[6] Pozzi M, Aung M S H, Zhu M, Jones R K and Goulermas J Y 2012 The pizzicato knee-joint energy harvester: characterization with biomechanical data and the effect of backpack load Smart Mater. Struct. 21 075023

[7] Ylli K, Hoffmann D, Willmann A, Becker P, Folkmer B and Manoli Y 2015 Energy harvesting from human motion: exploiting swing and shock excitations Smart Mater. Struct. 24 025029

[8] Gu L and Livermore C 2011 Impact-driven, frequency up-converting coupled vibration energy harvesting device for low frequency operation Smart Mater. Struct. 20 045004

[9] Umeda M, Nakamura K and Ueha S 1996 Analysis of the Transformation of Mechanical Impact Energy to Electric Energy Using Piezoelectric Vibrator Jpn. J. Appl. Phys. 35 3267–73

[10] Renaud M, Fiorini P, van Schaijk R and van Hoof C 2009 Harvesting energy from the motion of human limbs: the design and analysis of an impact-based piezoelectric generator Smart Mater. Struct. 18 035001

[11] Kulah H and Najafi K 2004 An electromagnetic micro power generator for low-frequency environmental vibrations Micro Electro Mechanical Systems, 2004. 17th IEEE International Conference on (MEMS) (IEEE) pp 237–40

[12] Rastegar J, Pereira C and Nguyen H-L 2006 Piezoelectric-based power sources for harvesting energy from platforms with low-frequency vibration Smart Structures and Materials 2006: Industrial and Commercial Applications of Smart Structures Technologies vol 6171, ed E V White (San Diego, CA, USA: SPIE) pp 617101–7

[13] Luong H T and Goo N S 2012 Use of a magnetic force exciter to vibrate a piezocomposite generating element in a small-scale windmill Smart Mater. Struct. 21 025017

[14] Pillatsch P, Yeatman E M and Holmes A S 2014 Magnetic plucking of piezoelectric beams for frequency up-converting energy harvesters Smart Mater. Struct. 23 025009

[15] McCullagh J J, Galchev T, Peterson R L, Gordenker R, Zhang Y, Lynch J and Najafi K 2014 Long-term testing of a vibration harvesting system for the structural health monitoring of bridges Sensors and Actuators A: Physical 217 13950

[16] Pillatsch P, Yeatman E M and Holmes A S 2012 A scalable piezoelectric impulse-excited energy harvester for human body excitation Smart Materials and Structures 21 115018

[17] Sato T and Igarashi H 2015 A chaotic vibration energy harvester using magnetic material Smart Mater. Struct. 24 025033

[18] Wickenheiser A M and Garcia E 2010 Broadband vibration-based energy harvesting improvement through frequency up-conversion by magnetic excitation Smart Mater. Struct. 19 065020

[19] Mann B P and Owens B A 2010 Investigations of a nonlinear energy harvester with a bistable potential well J. Sound Vib. 329 1215–26

[20] Pozzi M and Zhu M 2012 Characterization of a rotary piezoelectric energy harvester based on plucking excitation for knee-joint wearable applications Smart Mater. Struct. 21 055004

[21] Pozzi M, Almond H J, Leighton G J T and Moriarty R J 2015 Low-profile and wearable energy harvester based on plucked piezoelectric cantilevers Proc. SPIE Smart Sensors, Actuators, and MEMS VII; and Cyber Physical Systems vol 9517 (Barcelona (Spain)) pp 951706–951706 – 9

[22] Diedrich F J and Warren W H Jr 1995 Why change gaits? Dynamics of the walk-run transition J. Exp. Psychol. Hum. Percept. Perform. 21 183–202

[23] Riemer R and Shapiro A 2011 Biomechanical energy harvesting from human motion: Theory, state of the art, design guidelines, and future directions Journal of NeuroEngineering and Rehabilitation 8 22